EPTT 2024
Escola de Primavera de Transição e Turbulência

ABCM
Associação Brasileira de Engenharia e Ciências Mecânicas

EPTT-2024-0050
Turbulent Channel flow with Coriolis force using Large-Eddy Simulation

Igor Augusto de Melo
Escola de Engenharia de São Carlos - Universidade de São Paulo
Av. Trabalhador São Carlense, 400
13566-590, São Carlos - SP
igor_amelo@usp.br

Livia S. Freire
Leandro Franco de Souza
Instituto de Ciências Matemáticas e de Computação - Universidade de São Paulo
Av. Trabalhador São Carlense, 400
13566-590, São Carlos - SP
liviafreire@usp.br, lefraso@icmc.usp.br

Matheus Tozo de Araujo
Instituto Federal do Paraná
R. Cariris, 750
85760-000, Capanema - PR
matheus.araujo@ifpr.edu.br

Abstract. *In this study, Large-Eddy Simulation (LES) was employed to investigate the behavior of the flow in a turbulent half-channel subjected to Coriolis force at different rates (rotation rates 0, 0.018, 0.054, 0.091). The results obtained were compared to Direct Numerical Simulations (DNS) of the Poiseuille-Ekman flow for the same rotation rates. Two subgrid-scale models were tested in the non-rotating case, and the Lagrangian-Averaged Scale-Invariant (LASI) method was selected due to its superior proximity to the DNS results. The LES simulations followed the statistics behavior observed in DNS, and confirmed a reduction in turbulence as the non-inertial Coriolis force increased. This finding was validated through the analysis of turbulence kinetic energy, Reynolds shear stress and average velocity profiles compared to DNS data.*

Keywords: *Turbulent flows, Atmospheric boundary-layer, Large-Eddy Simulations, Coriolis*

1. INTRODUCTION

Understanding and accurately modeling turbulence effects in flows remains a critical challenge for scientists and engineers. This type of phenomenon plays an essential role in various natural processes, especially those present in the atmosphere, from the transportation of pollutants to the operation of wind turbines. Among the computer models used to simulate turbulent flows, Large-Eddy Simulation (LES) has emerged as a valuable tool, combining precision with computational efficiency. This study aims to advance this knowledge by employing LES to evaluate the behavior of turbulent rotating half-channel flows, which are crucial in atmospheric dynamics and engineering applications.

LES is an essential tool in aeronautical applications. It allows us to simulate the large scales of turbulent flows in complex geometric configurations, such as those found in aircraft components (Moreau, 2019) and wind turbines (Yang *et al.*, 2014). It stands out in situations where the complete simulation of all turbulent scales proves unfeasible due to the high computational demand of a very refined mesh (Romanelli *et al.*, 2023). This facilitates the detailed investigation of phenomena that were difficult to study experimentally. By employing the use of LES, it becomes feasible to predict noise levels and optimize projects before their physical construction, thus showing the potential of LES to improve engineering practices (Tyacke *et al.*, 2017).

When modeling atmospheric flows, it is crucial to consider the presence of Coriolis effects, especially on significant geophysical scales. Therefore, incorporating these forces into the computer simulation is necessary for an analysis of the observed phenomena. We aim to broaden the understanding of these results, using LES as the main tool and comparing it

with the results of previous research using Direct Numerical Simulation (DNS), which solves the Navier-Stokes equations without having to use turbulence models, encompassing all the spatial and temporal scales of turbulence.

This article explores how LES is used to predict turbulent channels under the effect of non-inertial forces (Coriolis Force), as present in the atmosphere due to the Earth's rotation. The study is built on previous research (Mehdizadeh and Oberlack, 2010) conducted with analytical and numerical methods using DNS, which revealed the sensitivity of turbulent effects to rotation. This paper will be used as a starting point for our research, providing valuable information on the dynamics of these flows using less computing power.

2. MATHEMATICAL FORMULATION

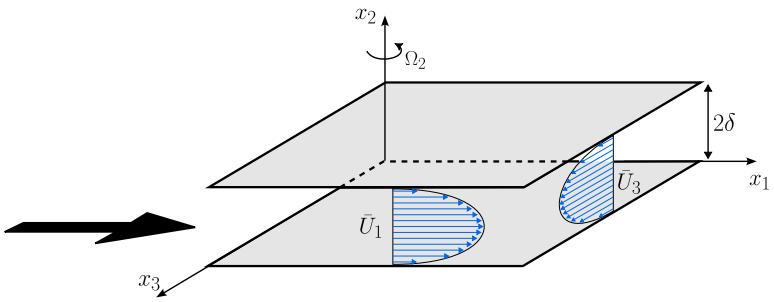

Figure 1. Domain geometry of a channel flow under Coriolis non-inertial force.

In this article, we will work with the hypothesis of a Newtonian, incompressible, three-dimensional fluid flow. The governing equations of the problem that act over the domain described in Fig. 1 are the Navier-Stokes equations with the presence of the Coriolis force (Mehdizadeh and Oberlack, 2010),

$$\frac{\partial u_i}{\partial t} + u_j \frac{\partial u_i}{\partial x_j} = -\frac{\partial p}{\partial x_i} + \frac{1}{\mathrm{Re}_{\tau 0}} \frac{\partial^2 u_i}{\partial x_j^2} - \epsilon_{ijk}\,\mathrm{Ro}_j\, u_k, \tag{1}$$

$$\frac{\partial u_i}{\partial x_i} = 0, \tag{2}$$

where u_i is the flow velocity in the direction x_i, p is pressure, $Re_{\tau 0}$ is the Reynolds number based on the friction velocity in the simulation without rotation, Ro_j is the rotation number in the direction x_j and ϵ_{ijk} is the unitary permutation tensor. The Rotation and Reynolds numbers are defined, respectively, as

$$\mathrm{Ro}_j = \frac{2\Omega_j \delta}{U_{\tau 0}} \quad \text{and} \quad \mathrm{Re}_{\tau 0} = \frac{U_{\tau 0}\delta}{\nu}, \tag{3}$$

where δ is the half-channel height, Ω_j is the axis angular velocity, ν is the kinematic viscosity of the fluid and $U_{\tau 0}$ is the friction velocity in the case without rotation.

2.1 Filtered Navier-Stokes Equations

The LES code used in this study is based on the model described by Freire and Chamecki (2021) and Bou-Zeid *et al.* (2005) for the atmospheric boundary layer. This model incorporates a sub-grid scale (SGS) approach to capture the effects of small turbulence scales that are not explicitly resolved in the simulation. The mathematical formulation of the problem is presented below.

Decomposing the simulation velocity into resolved and subgrid scale components, we have:

$$u_i = \widetilde{u_i} + u_i'', \tag{4}$$

where $\widetilde{u_i}$ is the filtered part of the velocity that was numerically solved by the mesh of our computational domain, and u_i'' is the residual part, i.e., unresolved (also called Subgrid Scale, or SGS). The filtered velocity field $\widetilde{u_i}$ represents the motion of large-scale vortices. It should be noted here that despite being analogous to Reynolds decomposition, generally the residual filtered is not zero, i.e.,:

$$\widetilde{u_i''} \neq 0. \tag{5}$$

The scales of the domain are defined by a low-pass filter in the spectrum domain to the exact solution (Sagaut, 2005). The generalized operation of a filter applied over a space-time variable $U(\boldsymbol{x},t)$ is a convolution product described in the physical space as:

$$\bar{U}(\boldsymbol{x},t) = \int_{-\infty}^{+\infty}\int_{-\infty}^{+\infty} U(\boldsymbol{\xi},t')\,G(\boldsymbol{x}-\boldsymbol{\xi},t-t')\,dt'd^3\boldsymbol{\xi} \quad \xrightarrow{\text{denoted by}} \quad \bar{U} = G * U, \tag{6}$$

where the integration is done over the entire flow domain, and the filter function satisfies the conditions:

- conservation of constants

$$\bar{u} = u \Longleftrightarrow \int_{-\infty}^{+\infty}\int_{-\infty}^{+\infty} G(\boldsymbol{\xi},t')\,d^3\boldsymbol{\xi}dt' = 1$$

- linearity

$$\overline{\phi+\psi} = \bar{\phi}+\bar{\psi}.$$

- commutation

$$\overline{\frac{\partial\phi}{\partial s}} = \frac{\partial\bar{\phi}}{\partial s}, \quad s = \boldsymbol{x},t$$

Therefore, applying the filtering operator to the Navier-Stokes equations (1), we obtain the following filtered equations:

$$\begin{aligned}
&\frac{\partial\widetilde{u_i}}{\partial t} + \frac{\partial\widetilde{u_iu_j}}{\partial x_j} = -\frac{1}{\rho}\frac{\partial\widetilde{p}}{\partial x_i} + \nu\frac{\partial^2\widetilde{u_i}}{\partial x_j\partial x_j} + F_i,\\
&\frac{\partial\widetilde{u_i}}{\partial x_i} = 0.
\end{aligned} \tag{7}$$

The nonlinear term $\widetilde{u_iu_j}$ is decomposed as:

$$\widetilde{u_iu_j} = \widetilde{u_i}\widetilde{u_j} + \tau_{ij}^R, \tag{8}$$

where τ_{ij}^R is the residual stress tensor that carries the effects of smaller scales (filtered) on the resolved scales $\widetilde{u_i}$. In other words, the effects of ${u_i}''$ on $\widetilde{u_i}$. Also, defining the residual turbulence kinetic energy as $e^R = \frac{1}{2}\tau_{ii}^R$, we can write

$$\widetilde{u_iu_j} = \tau_{ij} + \frac{2}{3}e^R\delta_{ij} + \widetilde{u_i}\widetilde{u_j}, \tag{9}$$

where τ_{ij} represents the anisotropic component of the residual stress tensor (or the deviatoric part), also known as the subgrid-scale (SGS) stress tensor:

$$\tau_{ij} = \tau_{ij}^R - \frac{2}{3}e^R\delta_{ij}. \tag{10}$$

The fundamental equations governing turbulent flow in LES are the incompressible filtered Navier-Stokes equations. These equations describe the dynamics of the resolved scale flow, incorporating the effects of subgrid-scale stresses:

$$\begin{aligned}
&\frac{\partial\widetilde{u_i}}{\partial t} + \frac{\partial\widetilde{u_i}\widetilde{u_j}}{\partial x_j} = -\frac{1}{\rho}\frac{\partial\widetilde{p}^*}{\partial x_i} + \nu\frac{\partial^2\widetilde{u_i}}{\partial x_j\partial x_j} - \frac{\partial\tau_{ij}}{\partial x_i} + F_i,\\
&\frac{\partial\widetilde{u_i}}{\partial x_i} = 0,
\end{aligned} \tag{11}$$

where $\widetilde{u_i}$ are the filtered velocity components, $\widetilde{p}^* = \widetilde{p} + \frac{2}{3}\rho e^R$ is the filtered modified pressure and F_i is the external body force. The SGS models are described next.

2.2 The Lagrangian-averaged Scale-invariant Model

In the work by Bou-Zeid *et al.* (2005), a scale-invariant dynamic SGS model was proposed and tested, which is based on Lagrangian time averaging. This approach was applied to LES simulations operating at high Reynolds numbers on both homogeneous and heterogeneous rough surfaces, and is an extension of Smagorinsky's Lagrangian dynamic model, in which measurements are accumulated over time following the flow path of the resolved velocity field. In the present study, this model will be compared to the Scale-Dependent method, which introduces a scale dependency in the Smagorinsky coefficient through an additional test filtering operation at a new coarser scale, determining how the coefficient varies as a function of the mesh scale.

A few considerations must be taken into account regarding the use of this models in this work. Although we're using a relatively low Reynolds number ($Re_{\tau 0} = 180$), and turbulence may be less intense, it still plays a significant role in the flow. As will be demonstrated in the results section, this model accurately predicts the behavior of the turbulent flow, making it suitable for the Reynolds number used here.

2.2.1 Smagorinsky-Lilly Model

The most popular model for SGS is based on eddy-viscosity and mixing length theory. The Smagorinsky-Lilly SGS model gives us an approximation for the SGS stress tensor as:

$$\tau_{ij}^{\mathrm{SMAG}} = -2\nu_T \widetilde{S}_{ij} = -2(c_s\Delta)^2 |\widetilde{S}| \widetilde{S}_{ij}, \tag{12}$$

where ν_T is the eddy viscosity, c_s is the Smagorinsky coefficient, Δ is the filter width scale, $\widetilde{S}_{ij} = \frac{1}{2}\left(\frac{\partial \widetilde{u}_i}{\partial x_j} + \frac{\partial \widetilde{u}_j}{\partial x_i}\right)$ is the strain rate tensor of the resolved velocity field, and $|\widetilde{S}| = \sqrt{2\widetilde{S}_{ij}\widetilde{S}_{ij}}$ is the magnitude of the strain rate.

2.2.2 Dynamic Model and Scale dependence factor

As described in Germano *et al.* (1991), the Dynamic Model uses the smallest resolved scales to calculate the model coefficient throughout the simulation. It is based on the SGS stress relation, using Germano's identity to relate the subgrid stresses at different scales:

$$L_{ij} = T_{ij} - \widehat{\tau}_{ij}, \quad \text{where} \quad L_{ij} = \widehat{\widetilde{u}_i\widetilde{u}_j} - \widehat{\widetilde{u}}_i\widehat{\widetilde{u}}_j, \quad \text{and} \quad T_{ij} = \widehat{\widetilde{u}_i\widetilde{u}_j} - \widehat{\widetilde{u}}_i\widehat{\widetilde{u}}_j, \tag{13}$$

where L_{ij} is the tensor defined from the intermediate scales between Δ and $\alpha\Delta$, T_{ij} is the subgrid stresses in the test filter $\widehat{\Delta} = \alpha\Delta = 2\Delta$. The Fig. 2 illustrates the identity.

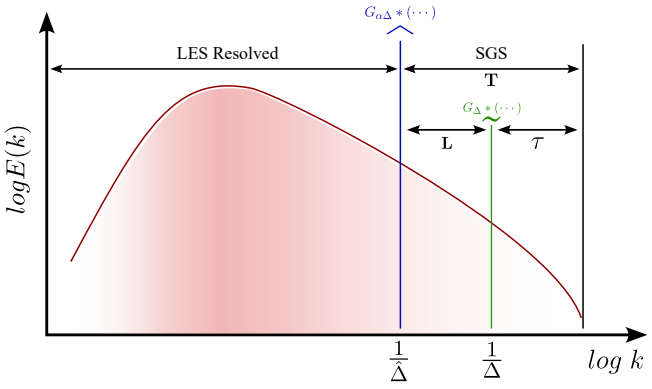

Figure 2. Sketch of the turbulence energy spectrum showing the wavenumbers corresponding to the filter scales Δ and the test-filter scale $\alpha\Delta$. The vertical lines represent the action of the spectrally sharp cutoff filter.

Applying the Smagorinsky model to work out the deviatoric parts of the subgrid stresses on the Δ and $\widehat{\Delta}$ scales:

$$\widehat{\tau}_{ij} = -2(c_{s,\Delta}\Delta)^2 \widehat{|\widetilde{S}|\widetilde{S}_{ij}}, \quad T_{ij} = -2(c_{s,\widehat{\Delta}}\widehat{\Delta})^2 \widehat{|\widetilde{S}|}\widehat{\widetilde{S}}_{ij} \tag{14}$$

The resulting expression of Germano's identity produces an error $\epsilon_{ij} = L_{ij} - (T_{ij} - \widehat{\tau}_{ij})$ due to the Smagorinsky model:

$$\epsilon_{ij} = L_{ij} - 2(c_{s,\Delta}\Delta)^2 \left(\widehat{|\widetilde{S}|\widetilde{S}_{ij}} - (\alpha\beta)^2 \widehat{|\widetilde{S}|}\widehat{\widetilde{S}}_{ij}\right) = L_{ij} - c_{s,\Delta}^2 M_{ij} \tag{15}$$

were $\beta = \dfrac{c_{s,\widehat{\Delta}}}{c_{s,\Delta}}$ is the scale dependence and $M_{ij} = 2\Delta^2 \left(\widehat{|\widetilde{S}|\widetilde{S}_{ij}} - (\alpha\beta)^2 \, \widehat{|\widetilde{S}|}\widehat{\widetilde{S}}_{ij} \right)$. In the case where $\beta = 1$ or $c_{s,\alpha\Delta} = c_{s,\Delta}$, the model exhibits scale invariance, known as LASI model (Lagrangian-Averaged Scale-Invariant model). Otherwise, it reflects scale dependence, referred to as LASD (Lagrangian-Averaged Scale-Dependent model).

To minimize the error ϵ_{ij} in the sense of least squares minimization of $\langle e_{ij} e_{ij} \rangle$ an approximation for the coefficient of is used:

$$c_{s,\Delta}^2 = \frac{\langle L_{ij} M_{ij} \rangle}{\langle M_{ij} M_{ij} \rangle}, \tag{16}$$

where $\langle\ \rangle$ represents averaging.

2.2.3 Lagrangian Average

The dynamic Smagorinsky coefficient is obtained along fluid trajectories, instead of a fixed spatial average. It is calculated by minimizing the weighted temporal average along the $e_{ij} e_{ij}$ error trajectories:

$$E = \int_{-\infty}^{t} e_{ij} \left[\mathbf{z}(t'), t' \right] e_{ij} \left[\mathbf{z}(t'), t' \right] W(t - t') \, dt', \tag{17}$$

where $\mathbf{z}(t')$ is the previous position of the fluid particle and $W(\tau)$ is the weight function. Thus, by differentiating with respect to $c_{s,\Delta}^2$ and setting it equal to zero:

$$c_{s,\Delta}^2 = \frac{\mathcal{J}_{LM}}{\mathcal{J}_{MM}}, \quad \text{where} \quad \mathcal{J}_{AB} = \int_{-\infty}^{t} A_{ij} B_{ij} \left[\mathbf{z}(t'), t' \right] W(t - t') \, dt. \tag{18}$$

The LASD model was validated in DNS simulations of high-Reynolds boundary layer flows over rough walls (Bou-Zeid *et al.*, 2005), showing good dissipation characteristics when compared to other SGS models, such as the Smagorinsky-Lilly model with a wall-damping function (super dissipative) and the scale-invariant dynamic model (subdissipative). However, for the low-Reynolds case in this study, the LASI model provided better results, as it will be shown later.

2.3 Boundary Conditions and Initialization

LES simulations were initialized with velocity data obtained from a previous high-Reynolds number simulation of the same domain, in order to avoid relaminarization of the flow. Boundary conditions are periodic in the horizontal directions. Due to the vertically staggered grid, the bottom boundary condition correspond to zero vertical velocity at the wall and $u^+ = y^+$ for the horizontal velocity components, which are located at the center of the first grid point (inside the viscous sublayer). At the top boundary, zero vertical velocity and zero vertical gradient of horizontal velocities are employed.

3. NUMERICAL RESULTS

The LES simulation domain represents a half-channel with $Re_{\tau 0} = 180$, subjected to a range of Coriolis forces. The simulation parameters for the LES simulations are detailed in Table1, and the specifications of the domain for each case, DNS and LES, for all the Coriolis forces, are represented in Table 2.

3.1 Validation of the SGS Model

To validate the subgrid model that was used in the LES code, a non-rotational case was simulated for the LASI and LASD cases, so the better model could be selected for the final results. Figures 3 – 5 show the results compared to the DNS, and the use of LASI SGS model can be justified by the proximity of its results to the DNS data, as can be noticed by the velocity profile and turbulence kinetic energy (TKE) results. We hypothesize that the need for a second filter in the LASD model, which in theory should also be in the inertial scales of the flow, may be affected by the low-Reynolds number used here.

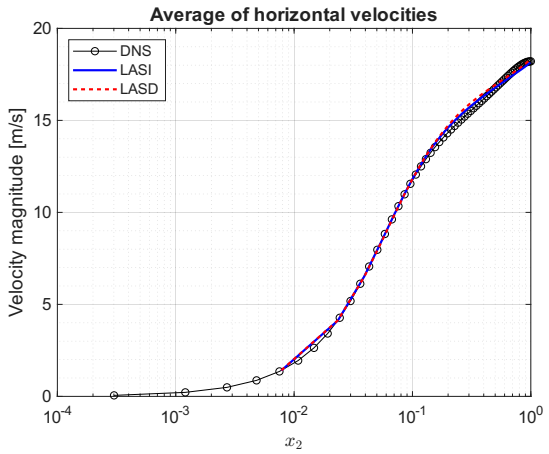

Figure 3. Horizontal velocities magnitudes for the SGS models.

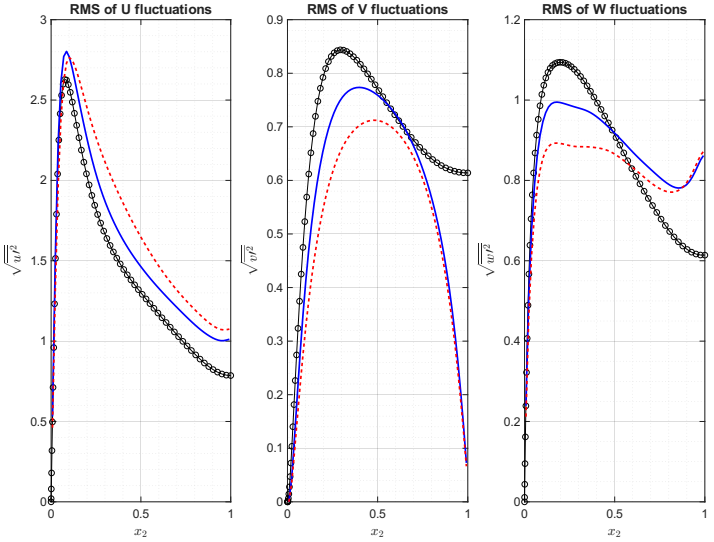

Figure 4. RMS value of the velocity fluctuations for different SGS models at $Re_{\tau 0} = 180$

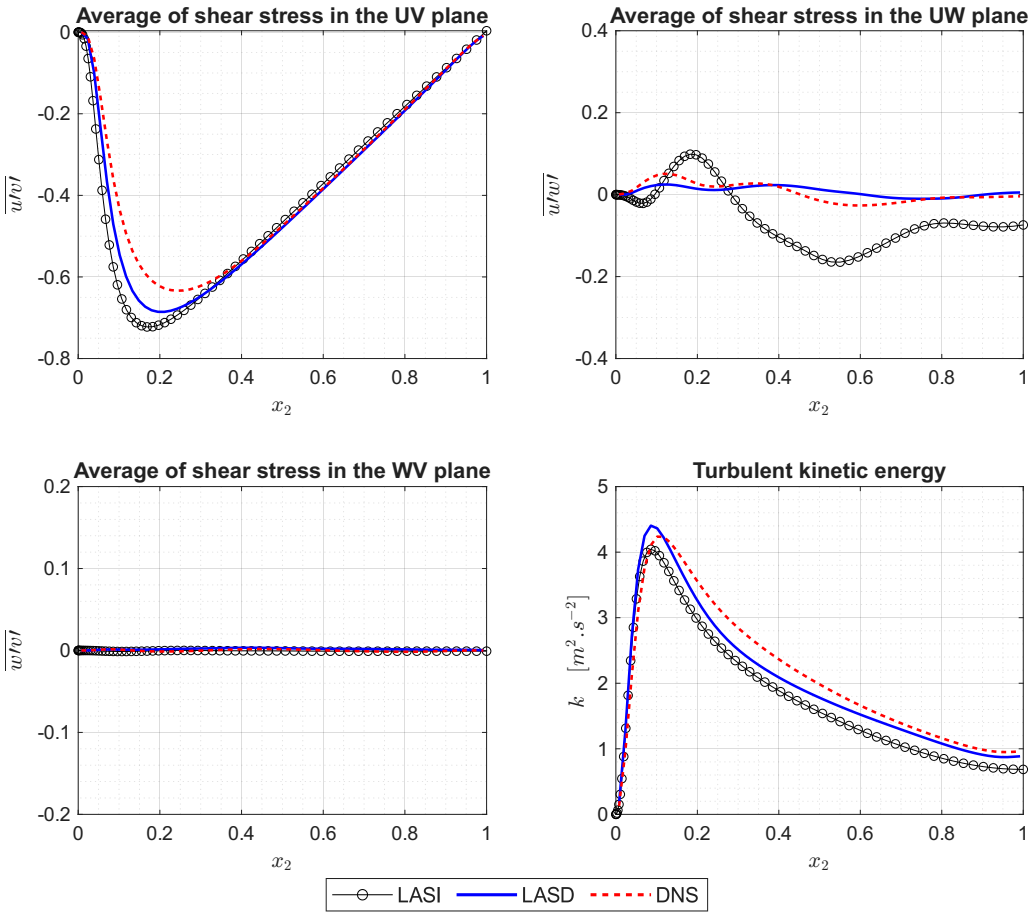

Figure 5. Turbulent shear stresses and turbulent kinetic energy for different SGS models at $Re_{\tau 0} = 180$

3.2 Final LES Simulation Results

The final results are presented in Figures 6 – 9, and they show the expected behavior of change in flow statistics with the increase of Coriolis force, as described by Mehdizadeh and Oberlack (2010) using DNS.

Figure 6 shows the mean streamwise horizontal velocity profiles, where LES results closely match the DNS data,

Mean pressure gradient force ($F_i = \langle(1/\rho)(d\bar{p}/dx), 0, 0\rangle$)	$\langle {U_{\tau 0}}^2/\delta, 0, 0\rangle$
Simulation time step (Δt)	$0.0002\delta/U_{\tau 0}$
Number of simulation time steps (N_t)	200 000

Table 1. Simulation parameters for LES ($\delta = 1$ and $U_{\tau 0} = 1$).

especially near the wall. However, discrepancies are observed further from the wall, particularly at the non-rotation case. This deviation is attributed to the limitations in capturing finer turbulence scales due to the coarser grid resolution in LES compared to DNS.

Figures 7 presents the root-mean-square (RMS) of velocity fluctuations. LES captures the qualitative trends observed in DNS, such as the reduction in turbulence intensity with increasing rotation. However, the quantitative agreement diminishes with increasing distance from the wall, particularly in the spanwise and vertical direction, where LES underpredicts the fluctuations.

Model	Ro_2 **(rad)**	**Grid resolution** ($n_{x_1} \times n_{x_2} \times n_{x_3}$)	**Computational domain** ($x_1 \times x_2 \times x_3$)	**Flow state**
DNS	0	128 x 129 x 128	$4\pi \times 2 \times 2\pi$	Turbulent
	0.018	128 x 129 x 384	$4\pi \times 2 \times 6\pi$	
	0.054	128 x 129 x 512	$4\pi \times 2 \times 8\pi$	
	0.091	128 x 129 x 384	$4\pi \times 2 \times 6\pi$	
LES	0	64 x 64 x 64	$2\pi \times 1 \times 2\pi$	Turbulent
	0.018			
	0.054			
	0.091			

Table 2. Domain specifications for all simulations at $Re_{\tau 0} = 180$.

We found that even small rotation rates have a significant impact on the physical characteristics of the channel flow, such as the average velocity, generating relevant transverse flows. In addition, a decrease in turbulence was noticed with increasing rotation rate, leading to a transition from a turbulent state to an almost laminar state in some conditions described by Mehdizadeh and Oberlack (2010). This is due to the instability in the turbulent shear stress, resulting in the formation of elongated patterns similar to rotating vortices.

This study suggests that while LES with LASI model is effective in predicting near-wall dynamics, improvements in subgrid-scale modeling or grid resolution are necessary for better accuracy in the outer flow regions.

4. CONCLUSION

This research indicates that the LES is a robust tool to investigate the impact of rotation on the turbulent flow, in a much lower computational cost compared to the DNS. Our study indicates that increasing Coriolis force leads to a significant reduction in TKE. The qualitative agreement with DNS validates the LES approach for simulating rotating turbulent flows, although quantitative differences highlight areas for further refinement, specially in subgrid-scale modeling and grid resolution far away from the wall.

We intend to analyze in more depth how the interaction between turbulence, Coriolis forces, and flows in turbulent channels influence global dynamics. With this, we hope to contribute to a better understanding of turbulent processes in physical systems and, consequently, to the validation of more accurate and effective models of fluid behavior on various temporal and spatial scales.

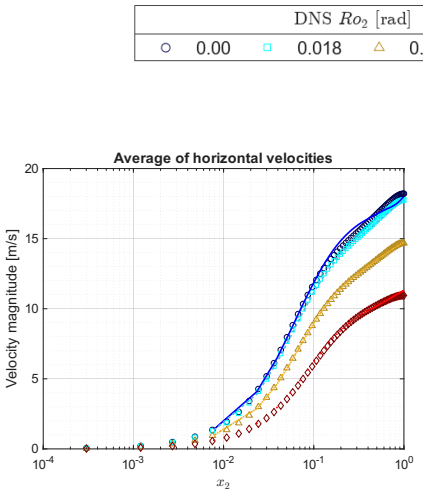

Figure 6. Horizontal velocity magnitudes for different rotation numbers (Ro_2) at $Re_{\tau 0} = 180$. DNS data from (Mehdizadeh and Oberlack, 2010), and LES data from this research.

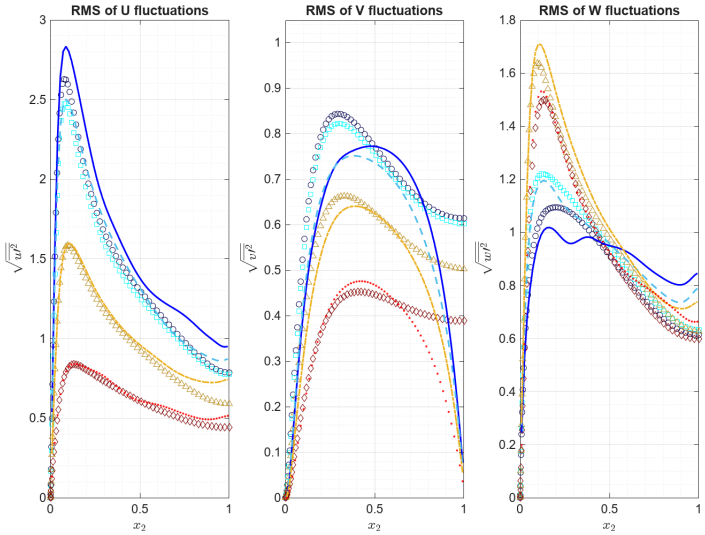

Figure 7. RMS values of the velocity fluctuation for different rotation numbers (Ro_2) at $Re_{\tau 0} = 180$

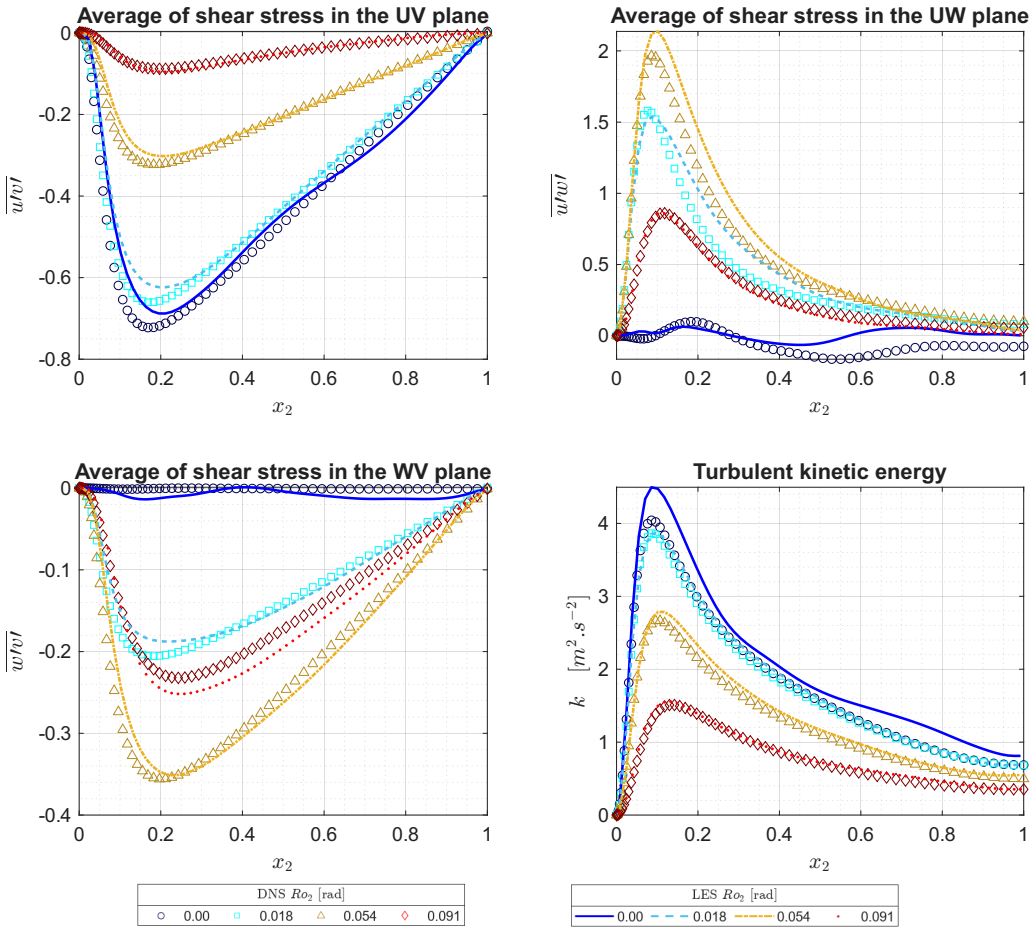

Figure 8. Turbulent shear stresses and turbulent kinetic energy for different rotation numbers (Ro_2) at $Re_{\tau 0} = 180$

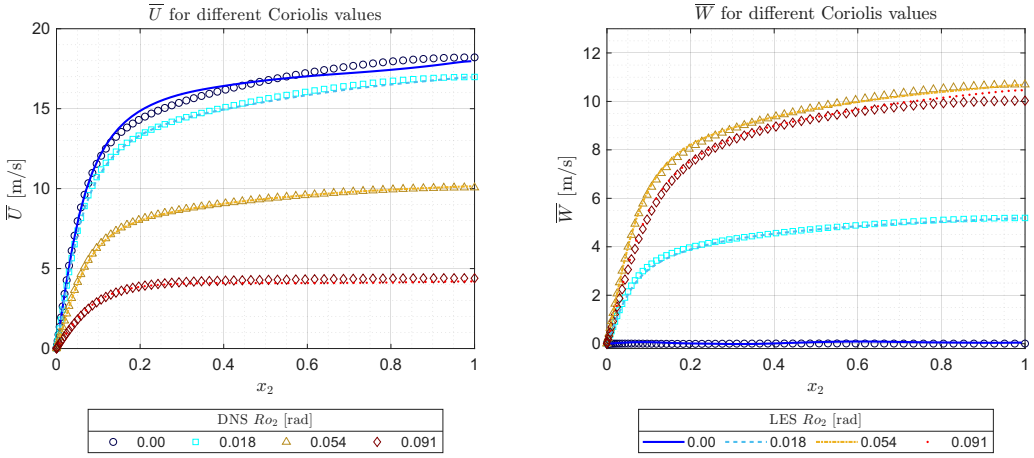

Figure 9. Mean velocities in the streamwise ($\overline{U}$) and the spanwise ($\overline{W}$) directions for different rotation numbers (Ro_2) at $Re_{\tau 0} = 180$

5. ACKNOWLEDGEMENTS

The authors acknowledge the University of São Paulo and the São Paulo Research Foundation (FAPESP processes 2018/24284-1 and 2023/12192-3) for financial support. Research carried out using the computational resource of the Center for Mathematical Applied to Industry (CeMEAI) funded by FAPESP (process number 2013/07375-0).

6. REFERENCES

Bou-Zeid, E., Meneveau, C. and Parlange, M., 2005. "A scale-dependent Lagrangian dynamic model for large eddy simulation of complex turbulent flows". *Physics of Fluids*, Vol. 17, No. 2, p. 025105. ISSN 1070-6631. doi: 10.1063/1.1839152. URL https://doi.org/10.1063/1.1839152.

Freire, L.S. and Chamecki, M., 2021. "Large-eddy simulation of smooth and rough channel flows using a one-dimensional stochastic wall model". *Computers Fluids*, Vol. 230, p. 105135. ISSN 0045-7930. doi:https://doi.org/10.1016/j.compfluid.2021.105135. URL https://www.sciencedirect.com/science/article/pii/S0045793021002735.

Germano, M., Piomelli, U., Moin, P. and Cabot, W.H., 1991. "A dynamic subgrid-scale eddy viscosity model". *Physics of Fluids A: Fluid Dynamics*, Vol. 3, No. 7, pp. 1760–1765. ISSN 0899-8213. doi:10.1063/1.857955. URL https://doi.org/10.1063/1.857955.

Mehdizadeh, A. and Oberlack, M., 2010. "Analytical and numerical investigations of laminar and turbulent Poiseuille–Ekman flow at different rotation rates". *Physics of Fluids*, Vol. 22, No. 10, p. 105104. ISSN 1070-6631. doi:10.1063/1.3488039. URL https://doi.org/10.1063/1.3488039.

Moreau, S., 2019. "Turbomachinery noise predictions: present and future". *Acoustics*, Vol. 1, pp. 92–116. doi: 10.3390/acoustics1010008.

Romanelli, M., Beneddine, S., Mary, I., Beaugendre, H., Bergmann, M. and Sipp, D., 2023. "Data-driven wall models for reynolds averaged navier–stokes simulations". *International Journal of Heat and Fluid Flow*, Vol. 99, p. 109097. ISSN 0142-727X. doi:https://doi.org/10.1016/j.ijheatfluidflow.2022.109097. URL https://www.sciencedirect.com/science/article/pii/S0142727X22001655.

Sagaut, P., 2005. *Large eddy simulation for incompressible flows: an introduction*. Springer Science & Business Media.

Tyacke, J., Naqavi, I., Wang, Z.N., Tucker, P. and Boehning, P., 2017. "Predictive Large Eddy Simulation for Jet Aeroacoustics–Current Approach and Industrial Application". *Journal of Turbomachinery*, Vol. 139, No. 8, p. 081003. ISSN 0889-504X. doi:10.1115/1.4035662. URL https://doi.org/10.1115/1.4035662.

Yang, X., Sotiropoulos, F., Conzemius, R., Wachtler, J. and Strong, M., 2014. "Large-eddy simulation of turbulent flow past wind turbines/farms: the virtual wind simulator (vwis)". *Wind Energy*, Vol. 18, pp. 2025–2045. doi:10.1002/we.1802.

7. RESPONSIBILITY NOTICE

The following text, properly adapted to the number of authors, must be included in the last section of the paper:
The authors are the only responsible for the printed material included in this paper.